# Nucleosome Arcs and Helices

## The nucleosome is a dynamic structure showing large conformational variability.

Jacques Dubochet and Markus Noll

*Summary.* Crystals and other regular arrangements of nucleosome cores have been obtained and analyzed in the electron microscope. Two types of regular structures have been studied in detail, the nucleosome arcs and cylinders. The latter are composed of concentric cylindrical layers of intertwined right-handed helices of nucleosome cores. These studies lead to the following conclusions and concepts. The overall structure of the nucleosome core is a short, wedge-shaped cylinder measuring about 110 by 110 by 60 angstroms. Nucleosome cores interact primarily between top and bottom planes. Nucleosome cores exhibit large conformational variability. A pivot allowing two degrees of rotational freedom is postulated in the region of the 70th base pair to account for this property of the nucleosome.

It has long been known that chromosomes are tight complexes of DNA and protein (*1*). While it was originally believed that the protein was the carrier of genetic information (*2*), the experiments of Avery (*3*) and the elucidation of DNA structure (*4*) established that all the genetic information was encoded in DNA. The recent discovery of nucleosomes (*5–8*) aroused new interest in the role of the chromosomal protein. An important characteristic of chromatin structure is the tightly packed state of DNA: a 100- to 10,000-fold contraction is required to fold the long DNA molecules into chromosomes. Although it is generally accepted that this is achieved by several orders of folding (*9*), at present only the first order may be described with reasonable precision and confidence (*6, 10, 11*). At this lowest level of organization, chromatin structure is based on a subunit (*5, 7, 8*), the nucleosome, which consists of two copies each of four of the five main types of histones (*12*), namely H2a, H2b, H3, and H4, and about 200 base pairs of DNA (*8, 13*) arranged on its outside (*11, 14, 15*) as originally proposed by Kornberg (*6*). Whereas in most cells the DNA size per nucleosome averages about 200 base pairs (*8, 13, 16, 17*), this length varies significantly between higher and lower eukaryotes (*18, 19*). Indeed, as was shown recently, variation of the DNA content of nucleosomes occurs also within the same type of cells or even within single cells (*20*). It appears, however, that all nucleosomes contain a conserved core (*18, 19, 21*) consisting of 140 base pairs of DNA believed to be associated more tightly with the histone octamer (*17–19, 21, 22*). These 140-base-pair nucleosome cores lack the fifth histone (*17, 22, 23*), histone H1, which is associated with the variable linker region and stabilizes the interaction of adjacent nucleosomes (*17*).

In our study of the structure of nucleosomes and their modes of interaction, we searched for conditions under which purified nucleosome cores aggregate into regular structures. Both hexagonal crystals and two-dimensional hexagonal associations of nucleosomes were obtained. Most frequently, however, two new types of ordered structures were observed—the cylinders and the arc-like arrays of nucleosomes. Their study revealed interactions between and within nucleosomes which may be important in maintaining higher orders of chromatin structure and which suggest a dynamic structure of the nucleosome well suited for its multiple physiological tasks (repression, activation, replication).

Dr. Dubochet was a research associate and Dr. Noll is an assistant professor in the Department of Cell Biology at the Biocenter of the University of Basel, Klingelbergstrasse 70, CH-4056 Basel, Switzerland. Dr. Dubochet's present address is EMBL, Postfach 10.2209, D-6900 Heidelberg, Germany.

### Purification of Nucleosome Cores

Micrococcal nuclease digestion of nuclei and subsequent purification of chromatin subunits in sucrose gradients (*8, 24*) made possible the preparation of nucleosomes on a scale sufficiently large for crystallization studies. However, the population of nucleosomes obtained by this procedure is heterogeneous and hence not suitable for crystallization. Several factors contribute to this heterogeneity. Some of them, like the variable content of DNA, histone H1, and nonhistone proteins of nucleosomes, may be removed by appropriate modifications of the purification procedure mentioned above. Other causes of heterogeneity, however, like the variation in histone modification or DNA sequences, are more difficult to eliminate. Therefore, we attempted to improve our preparation with respect to the first three factors only.

Extensive digestion of nuclei with micrococcal nuclease generates 10.6*S* nucleosomes, which contain a defined DNA size of 140 base pairs and which are devoid of histone H1 (*17, 22*). We selected conditions of micrococcal nuclease digestion to optimize homogeneity and yield of these 140-base-pair nucleosomes. The 140-base-pair nucleosomes were purified in sucrose gradients (Fig. 1) and concentrated by $MgCl_2$ precipitation. In a final purification step, traces of histone H1 and most nonhistone proteins were removed from the nucleosome cores by washing in 0.6*M* NaCl (*25*). These purified nucleosomes were used for crystallization and association experiments. They consisted of 140 base pairs of DNA and equimolar amounts of histones H2A, H2B, H3, and H4 but lacked histone H1 and most nonhistone proteins. Proteolysis was not detectable even after 5 weeks under associating conditions at room temperature (Fig. 1). Since up to 75 percent of the nucleosomes were present in ordered structures (*26*), it is obvious that these were also predominantly composed of undegraded histones and 140-base-pair DNA.

Analysis of the 140-base-pair nucleosomes in the electron microscope exhibited the familiar bead-like appearance. Shadow-casting of a freeze-dried preparation, however, revealed that most nucleosomes are attached in similar orientations to the supporting film and that the thickness of the nucleosome is only about half of its diameter of 110 Å (Fig. 2). Thus, the shape of the nucleosome core is more nearly a short cylinder than a sphere. This conclusion is in agreement with recent reports (*27–29*).


0036-8075/78/1020-0280$01.50/0 

### Hexagonal Crystals

In our attempts to obtain ordered aggregates of nucleosome cores, we chose conditions similar to those used for the crystallization of transfer RNA (*30*). Highly concentrated nucleosomes were equilibrated against micromolar concentrations of spermine and 9 percent isopropanol or 20 percent dioxan by dialysis or vapor diffusion. These conditions favor the regular arrangement of nucleosomes into hexagonal crystals (Fig. 3, a and b). In the projections observed most frequently, the characteristic concentration of the stain in the middle of the circular nucleosomes (*25, 28, 31*) was clearly visible (Fig. 3b), an indication that in this projection one is looking through rows of superimposed nucleosomes. The spacing of adjacent rows is 95 ± 4 Å. The dimensions of these crystals rarely exceeded 0.4 micrometers and hence the crystals were not suitable for analysis by x-ray diffraction.

Upon adhesion to hydrophilic supporting films or freshly cleaved mica, nucleosomes tend to pack in a two-dimensional hexagonal pattern (Fig. 3c). The distance between adjacent nucleosomes is 110 ± 4 Å. This value is slightly larger than the distance between the rows in the three-dimensional hexagonal crystals. The shrinkage of the crystals during dehydration could explain this difference.

In addition to the hexagonal crystals described previously (*27*), regular associations of nucleosomes resulted in two other types of arrangement. These were the arcs (Fig. 4) and the cylinders (Fig. 5). We now describe their structures and discuss possible implications for inter- and intranucleosomal interactions.

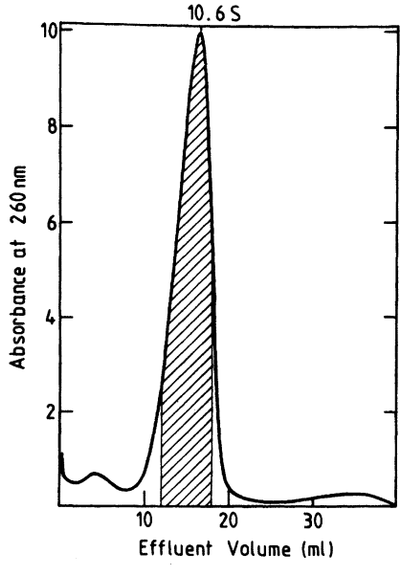


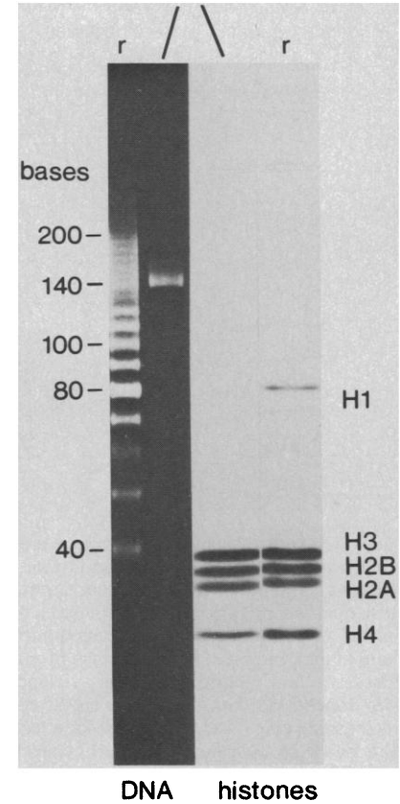


Fig. 1. Large-scale preparation and analysis of nucleosome cores. Rat liver nuclei were prepared as described (*5, 40*). Nuclei ($1.5 \times 10^8$/ml) were digested with micrococcal nuclease (60 unit/ml) in 0.34*M* sucrose, buffer A (15 m*M* tris-HCl, *p*H 7.4, 60 m*M* KCl, 15 m*M* NaCl, 15 m*M* 2-mercaptoethanol, 0.5 m*M* spermidine, 0.15 m*M* spermine), 0.5 m*M* PMSF, and 1 m*M* $CaCl_2$ for 20 minutes at 37°C. Digestion was stopped by the addition of 1/20 volume of 0.1*M* EDTA, *p*H 7. The nuclei were sedimented and then lysed in one-third of the original volume of 1 m*M* EDTA, *p*H 7. After centrifugation for 5 minutes at 2000 rev/min (Sorval GLC-1), the supernatant was removed and layered on isokinetic sucrose gradients (*24*). The analysis of such a gradient after centrifugation (Beckman SW 27 rotor) at 4°C for 36.5 hours at 26,000 rev/min is shown in the top panel. The material of the monosome peak (shaded area) was collected and pooled from several gradients. The nucleosomes were precipitated with 10 m*M* $MgCl_2$. After centrifugation for 20 minutes at 10,000 rev/min (Sorval SS-34 rotor), the nucleosomal pellet was dissolved in 10 m*M* EDTA, *p*H 7 ($A_{260}$ = 80). Traces of Hl and most nonhistone proteins were washed off the nucleosomes by the addition of two volumes of 0.9*M* NaCl, 15 m*M* tris-HCl, *p*H 7.4, 0.75 m*M* PMSF, and subsequent centrifugation through a 0.5-ml sucrose cushion of 1*M* sucrose, 0.6*M* NaCl, 10 m*M* tris-HCl, *p*H 7.4, 0.5 m*M* PMSF (Beckman SW 50.1 rotor) for 49.5 hours at 50,000 rev/min. The nucleosomes were dissolved at a concentration of 188 $A_{260}$ unit/mil in 10 m*M* sodium cacodylate, *p*H 7.0, 0.2 m*M* PMSF, equilibrated against this buffer, and used for crystallization or association experiments. Analysis of the DNA and protein components of these nucleosomes after 5 weeks of association at room temperature is shown in the left and right panels, respectively. The DNA's of a deoxyribonuclease I digest of chromatin (*14*) and histones of native chromatin (*40*) are shown for reference (*r*) in the left and right lanes, respectively. DNA analysis was performed in an 8 percent polyacrylamide slab gel (*41*), and histone analysis in a SDS-18 percent polyacrylamide slab gel (*12*).

### Nucleosome Arcs

Suspensions of cylinders (Fig. 5) reveal, after adhesion to mica, arc-like arrays of nucleosomes that tend to associate concentrically (Fig. 4a). These arcs arise from a top-to-bottom association of the cylindrically shaped nucleosomes. This is deduced from the regularly spaced radial striation indicating a period of 55 ± 4 Å at the internal radius of an arc and from the arc width of about 110 Å. The curvature of an arc is explained best by a small angle $\phi$, the wedge angle, between top and bottom plane of the cylindrical nucleosome. Thus, in its side view the nucleosome is wedge-shaped.

Single arcs have an internal radius of 400 ± 40 Å. This value varies, however, over a wide range under the action of external forces. Thus, when several arcs are associated concentrically, the internal radius ranges between 200 and 600 Å. The spacing of the striation is constant and independent of the radius (Fig. 4b). Consequently, the wedge angle of the nucleosomes is inversely proportional to the radius of the arc and may be calculated for any given radius. It is 7.9° for single arcs and varies between 16° and 5° in concentrically associated arcs.

### Cylinders of Nucleosome Cores

After several weeks of association under standard conditions, up to 75 percent of the nucleosomes form hollow cylinders (Fig. 5). These exhibit a characteristic periodical structure and appear to consist of several concentric layers when viewed parallel to their axes (white arrows in Fig. 5). Their length may be as much as a few micrometers, their outside diameter varies between 700 and 2000 Å, and the diameter of the central hole is preferentially either 220 ± 30 Å or 370 ± 30 Å. Most of the cylinders are irregular, and a clear distinction between short irregular cylinders and unordered aggregates is impossible. In some preparations, however, many of the cylinders are long and regular.

The regular cylinders consist of concentric layers of rows of nucleosomes. In preparations that have been freeze-dried and shadow-cast with metal the rows are clearly visible at the surface of the cylin-

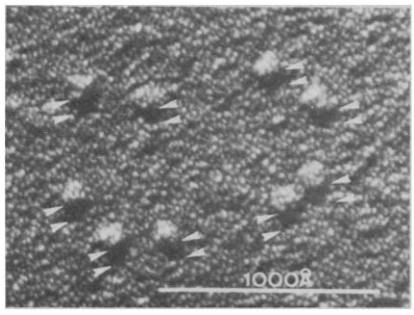


Fig. 2. Determination of the height of the nucleosome core by electron microscopy. Nucleosome cores were freeze-dried after adhesion to a hydrophilic carbon film (*42*). The specimen was shadow-cast with platinum and carbon from a source situated at an angle of 36° above the plane of the specimen. From the length of the shadow (marked by arrows), the height of the nucleosomes is found to be approximately 50 Å since the flattening of the nucleosomes is probably negligible in freeze-dried preparations.

ders (Fig. 6a); alternatively, in negatively stained preparations, they are visible at the edges of the cylindrical layers, permitting a tangential view of a small portion of the rows (Fig. 6, b and c). In other regions, the rows are not clearly resolved because of their superposition. In many cases the rows do not lie in a plane perpendicular to the cylinder axis but are tilted by an angle $\alpha$ (Fig. 6a). The width of the rows, about 90 Å (Fig. 6), suggests that they are constructed in a manner similar to the nucleosome arcs (Fig. 4), by a top-to-bottom assembly of the wedge-shaped cylindrical nucleosomes (*32*). This conclusion is confirmed by the regular striation of spacing, about 55 Å, along the rows, which is evident from an optical diffractogram of the central region of some cylinders (not shown). The striation is also observed directly, particularly at broken ends of cylinders (arrow in Fig. 6b).

The internal structure of the cylinders is partially revealed in negatively stained preparations. The closely packed rows are locally arranged in nearly hexagonal symmetry (Fig. 6, b and c). Although in some micrographs the order is conserved down to 30 Å, it is impossible to follow any single row of nucleosomes over more than a fraction of a turn because of the superposition of several rows. However, as is evident from the surface structure of freeze-dried cylinders (Fig. 6a) or from negatively stained preparations (Fig. 6, b and c), the organization of the rows is regular over large distances of the cylinders. Since any interruption of a row or a variation of its curvature radius or angle $\alpha$ would introduce irregularities, we conclude that the rows form closed circles or long helices of constant radius and pitch. For all cylinders examined in the freeze-dried preparations in which the rows were clearly tilted with respect to a plane perpendicular to the axis, the tilt was compatible only with a right-handed helical arrangement of the rows. In these cases, the angle $\alpha$ represents the pitch angle.

The pitch angle $\alpha$ of the external layer of different cylinders varies over a wide range. An estimate for its variability is obtained from freeze-dried (Fig. 6a) or, in favorable cases, from negatively stained cylinders (Fig. 6b). Thus, pitch angles between 0° and 25° to 30° have been measured. In the case of small angles $\alpha$, because of the relatively large errors of measurement, it cannot be ruled out that the cylinders consist of circular rows or even left-handed helices.

Figure 7 illustrates schematically the principal features of a typical cylinder consisting of three layers. The lower part of the cylinder shows a view of the external layer, as seen in Fig. 6a, whereas the upper part has been cut to reveal its internal structure. Each layer is composed of several intertwined helices consisting of nucleosome cores assembled by top-to-bottom association. Because the helices of one cylindrical layer run in the grooves of the adjacent layer or layers (Fig. 6, b and c), each layer consists of the same number of helices and all helices have the same pitch $p$. Therefore, the pitch angle $\alpha_1$, $\alpha_2$, and $\alpha_3$ of the external, intermediate, and internal layer, respectively, increases with decreasing radius. In general, $\alpha$ is related to the pitch of a helix with radius $r$ by the equation

$$\alpha = \arctan (p/2\pi r) \qquad (1)$$

Applying this relation to our measurements of the pitch angle of external layers, we find an upper limit of $\alpha \simeq 45°$ for the innermost layer (*33*).

The variation of $\alpha$ with the radius of the helices is verified qualitatively in Fig. 6b. The pitch angle $\alpha \simeq 15°$ of the out-

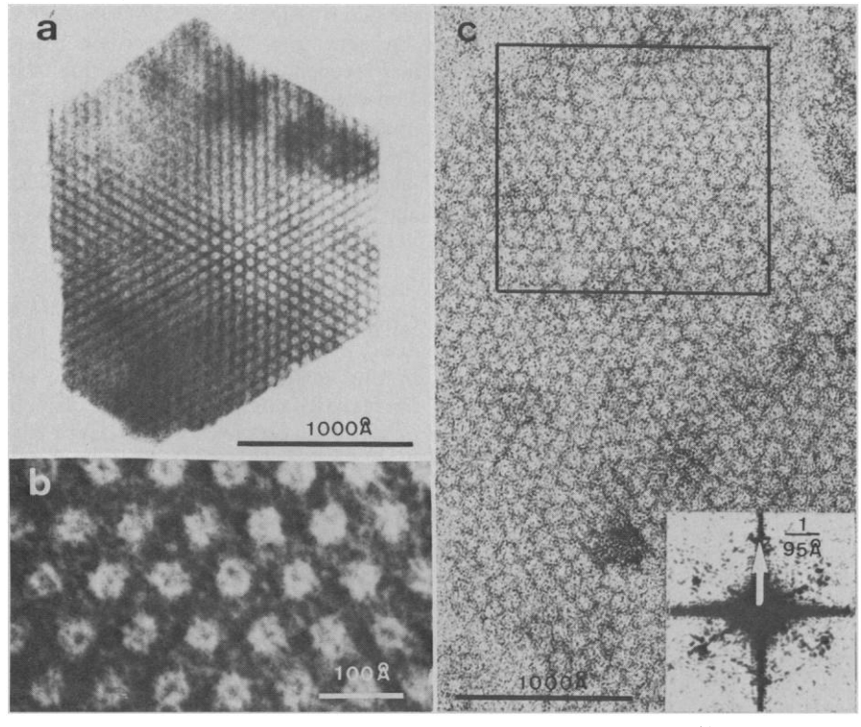


Fig. 3. (a) Hexagonal crystal of the nucleosome core. Crystals of nucleosome cores were obtained after 4 weeks of crystallization at room temperature in 10 m*M* sodium cacodylate, *p*H 6.1, 3 $\mu M$ spermine by vapor diffusion against 9 percent isopropanol. The initial concentration of the nucleosomes was 102 $A_{260}$ unit/ml. For electron microscopy, a portion was diluted tenfold in water. The specimen was prepared by adhesion to a hydrophilic film and stained with an aqueous solution of 1 percent uranyl acetate. The distance between adjacent rows of nucleosomes is 75 Å in this micrograph. In images recorded at low electron dose, this distance is 95 ± 4 Å (*43*). (b) Enlarged portion of (a). (c) Two-dimensional hexagonal packing of nucleosome cores. Two-dimensional juxtaposition of nucleosome cores was obtained from a tenfold dilution of a sample similar to the one described in Fig. 5 by adhesion to mica. For electron microscopy, the specimen was coated with carbon and floated on an aqueous solution of 2 percent uranyl acetate (*44*). The inset shows the optical diffractogram of the marked region.

ermost layer is measured at the broken end. From this measurement and the outer and inner radii (470 Å and 155 Å), the pitch angle for the innermost layer, calculated according to Eq. 1, is about 40°. This value is compatible with the observation of an angle $\alpha' = 40°$ (Fig. 6b) which corresponds to a pitch angle $\alpha \geqq 28°$ (*34*).

Another implication of the constant pitch for all helices of a cylinder is that the helical rows of nucleosomes get squeezed with decreasing radius. As illustrated in Fig. 8, this squeezing reduces the width $d$ of the helices with increasing pitch angle $\alpha$ according to $d = D \cos \alpha$. The displacement $D$ along the cylinder axis of adjacent helices is equal to the pitch $p$ divided by the number $n$ of interlaced helices per layer. In the typical example of the cylinder (Fig. 6b) in which $n = 9$ and $D = 91$ Å, the width $d$ of the helices of the inner- and outermost layer is reduced to 70 Å and 88 Å, respectively. Thus, nucleosome cores may undergo large conformational changes during their assembly into cylinders.

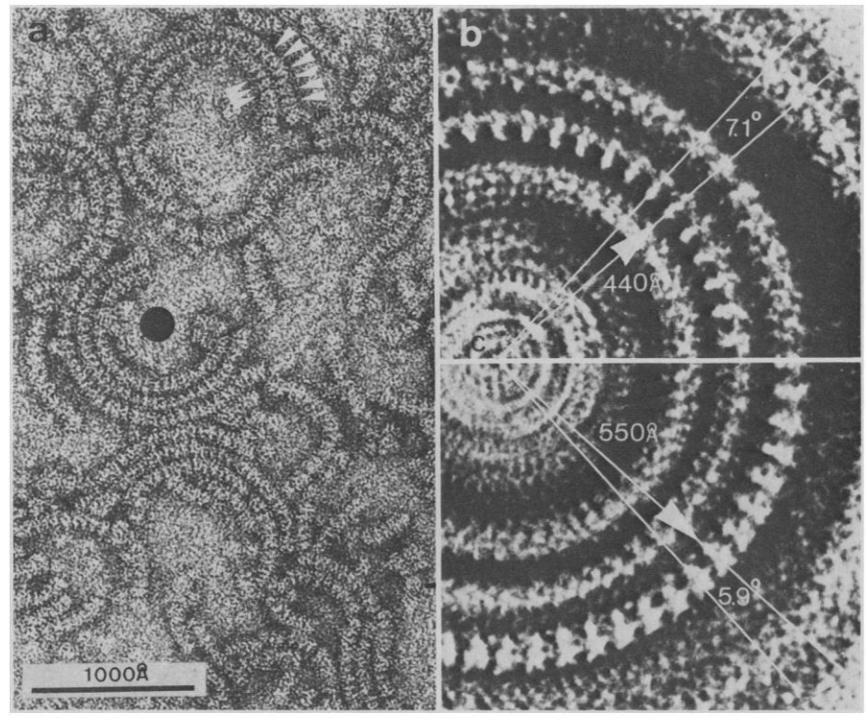


Fig. 4. (a) Nucleosome arcs. A specimen obtained from the solution described in Fig. 5 was prepared for electron microscopy as described in Fig. 3c. The arc width is about 110 Å, and direct measurement of the radial striation indicates a spacing of 50 to 60 Å (arrows). (b) Image processing of concentric arcs by Markham procedure (*45*). The three concentric arcs marked by a dot in Fig. 4a were used to reveal their periodicity more precisely by a Markham procedure (*45*). The pictures show the superposition of nine copies of the concentric arcs. In the upper panel, individual copies are rotated by an angle $\phi$ of 7.1° with respect to one another around the center $C$. This angle produces the largest amplification of the striation for the middle arc (internal radius = 440 Å). In the lower panel an angle of 5.9° that generates the strongest reinforcement of the striation for the outer arc (internal radius = 550 Å) was used. For both arcs the displacement at the internal radius is 55 Å.

## Conformational Variability

In our efforts to study the assembly of nucleosome cores into ordered structures, we have found hexagonal crystals, arcs, and cylinders. Whereas the hexagonal crystals are composed of nucleosomes of presumably identical shape, nucleosomes in arcs or cylinders exhibit a spectrum of different shapes. The overall structure of the nucleosome core resembles a wedge-shaped, short cylinder with a mean height of about 60 Å (Figs. 2 and 4) and a diameter of approximately 110 Å (Figs. 3, 4, and 6). These results confirm the structure deduced from x-ray analysis and electron microscopy of crystals (*27*). The existence of nucleosome arcs and cylinders indicates that this basic structure of the nucleosome core is not rigid but may show large changes in shape.

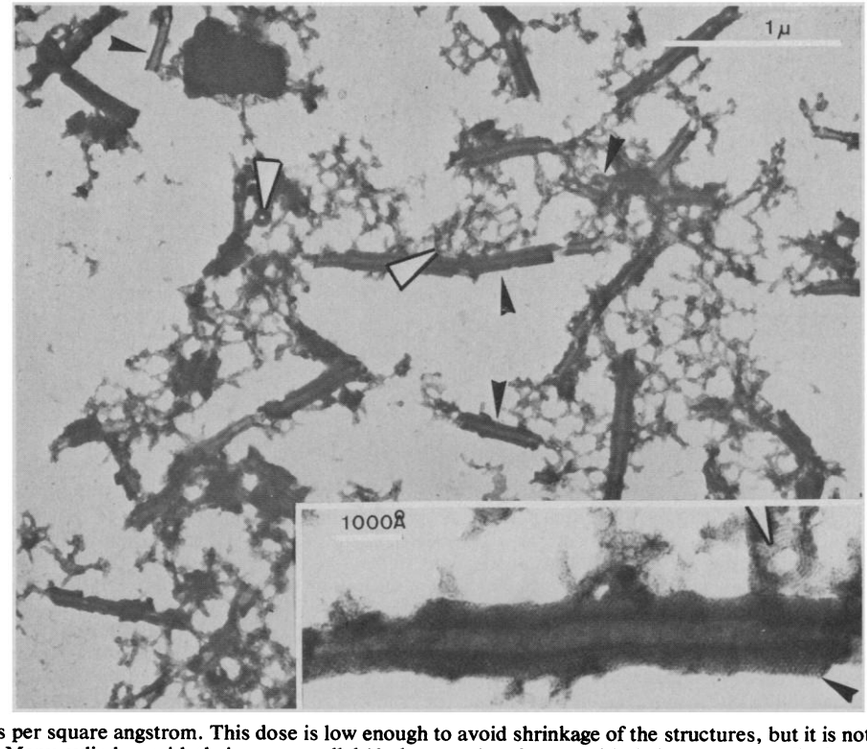


Fig. 5. View of a preparation of cylinders. Nucleosome cores ($A_{260} = 188$) were dialyzed against 10 m$M$ sodium cacodylate, $p$H 7.0, 11 $\mu M$ spermine, 9 percent isopropanol for 5 weeks at room temperature. For electron microscopy, the solution was diluted tenfold in water and negatively stained (after adhesion to a hydrophilic carbon film) with an aqueous solution of 2 percent uranyl acetate. The image was recorded with a total dose of 5 electrons per square angstrom. This dose is low enough to avoid shrinkage of the structures, but it is not sufficient to yield a sharp high-resolution image. Many cylinders with their axes parallel (dark arrows) and some with their axes perpendicular to the supporting film (white arrows) are visible. The insert shows an enlarged portion of the micrograph. It illustrates the periodical structure of the cylinder (dark arrow) and the concentric layers characteristic of cylinders with their axes perpendicular to the supporting film (white arrow).

In nucleosome arcs we observe a variability of the nucleosome structure that may be explained by a variation of the wedge angle $\phi$ altering between 5° and 16°. For cylinders consisting of helices of nucleosomes, the variability of $\phi$ is not sufficient to describe the entire spectrum of different shapes observed. This is evident from the following considerations. Each helical row of nucleosomes is characterized by its radius $r$ and its pitch angle $\alpha$ (Fig. 9). Such a helix may be built from wedge-shaped nucleosomes that are associated by top-to-bottom assembly. Assuming specific interactions at the interface of adjacent nucleosomes as in nucleosome arcs, we may generate a helix by rotating in each nucleosome the top and bottom planes with respect to one another. This rotation occurs around an axis passing through the centers of the top and bottom planes and results in the twist angle $\psi$ (Fig. 9). Thus, for small wedge angles $\phi$, the angles $\phi$ and $\psi$ are related to the observable parameters $\alpha$ and $r$ of a helix by the following approximations (*35*):

$$\phi = (h/r)\cos^2\alpha \quad (2)$$

and

$$\psi = (h/r)\sin\alpha\cos\alpha \quad (3)$$

in which $h$ denotes the mean height of the wedge-shaped cylindrical nucleosome. For a given cylinder, $\alpha$ and $r$ are not independent but related by Eq. 1.

From the observed variation of $\alpha$ and $r$, we may calculate the shape change of the nucleosome core according to Eqs. 2 and 3. Thus, we find that the largest distance by which the top and bottom planes move apart at the periphery of the nucleosome is 13 Å. In this case the two planes are not twisted with respect to one another, that is, $\psi = 0$. At the other extreme where the change of the twist angle $\psi$ is maximal, the displacement at the periphery of the nucleosome is 8 Å (*36*). Superimposed onto these movements is the squeezing effect mentioned above which is of similar magnitude.

An alternative explanation for the generation of helices of nucleosome cores by top-to-bottom assembly would be that the rotation by the angle $\psi$ occurs at the interface of adjacent nucleosomes rather than within the nucleosomes. However, this view could only replace the requirement for conformational variability due to changes of the twist angle $\psi$. Variability of the wedge angle $\phi$ would still need intranucleosomal movements. In addition, it appears more difficult to envision that the calculated relative movements of the order of 10 Å are restricted to the

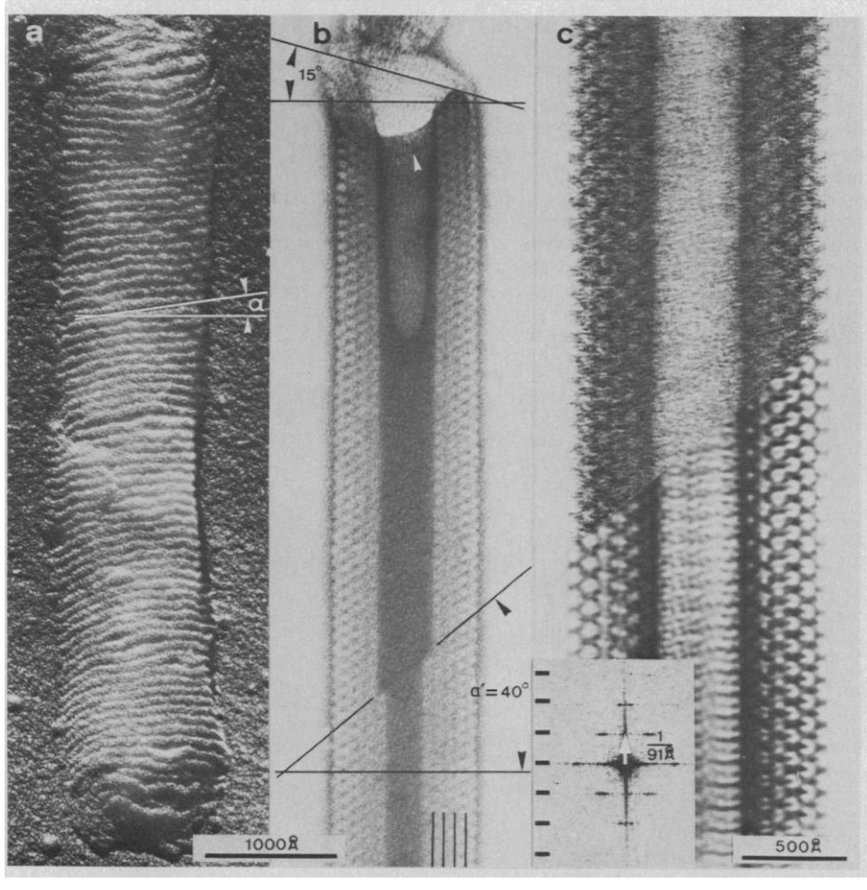


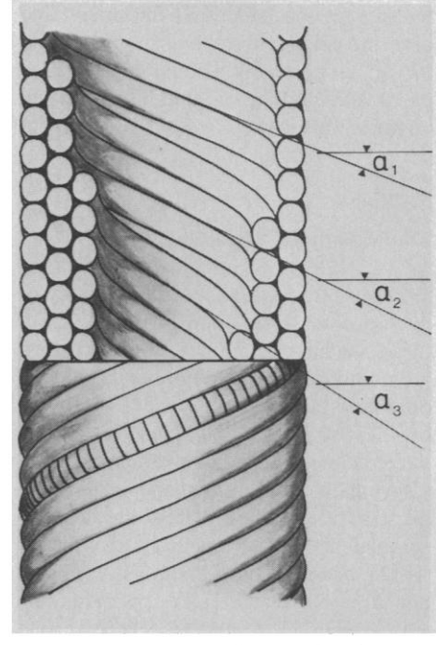


Fig. 6 (left). Regular cylinders of nucleosome cores. The specimens were obtained after 4 to 6 weeks of association as described (Fig. 5). (a) Freeze-dried cylinder. A preparation of cylinders was adsorbed to a positively charged film, freeze-dried (*42*), and shadow-cast. The source of the carbon-platinum evaporation was situated at an angle of 30° above the plane of the specimen. From the length of the shadow, it is deduced that the cylinder was considerably flattened upon adhesion to the supporting film. (b) Negatively stained cylinder. A preparation of cylinders was negatively stained with an aqueous solution of 2 percent uranyl acetate. The image was recorded with a low electron dose. The central hole of the cylinder was largely filled with stain, which prevented the cylinder from severe flattening. The cylinder consisted of four concentric layers in the upper part of the image, and a fifth layer at the inside of the lower part. The limits of the layers are indicated at the bottom of the micrograph. For the external layer, the pitch angle, $\alpha \simeq 15°$, is measured at the broken end of the cylinder because this layer is probably revealed by the stain between supporting film and cylinder (*46*). For the innermost layer, a lower limit of $\alpha$ can be deduced from the measured angle $\alpha' = 40°$ at the interruption of the layer (*34*). (c) Cylinder washed in water after negative staining. Washing the negatively stained cylinders in water removed most of the stain in the central hole. Because the electron dose used to record this micrograph was larger than that in (b), the radial shrinkage of the cylinder is also larger. The length of cylinders is not subjected to this effect and, thus, never reduced significantly. The optical filtration of the micrograph is shown in the lower part of the panel. It was generated by the use of the signal only along the seven layer lines marked in the optical diffractogram (shown in the inset). Fig. 7 (right). Schematic view of a cylinder. The lower part of the figure offers a view of the external layer of a cyliner (see Fig. 6a). Individual nucleosome codes are shown in one of the helices. In the upper part, a longitudinal section of the cylinder reveals its interior (see Fig. 6, b and c). The angles $\alpha_1$, $\alpha_2$, and $\alpha_3$ are the pitch angles of the external, intermediate, and internal layer, respectively.

narrow region at the interface than that they distribute over the entire nucleosome.

Our calculations are based on a model that assumes a rigid axis through the centers of the top and bottom planes of the nucleosome. Hence, the calculated values represent the minimal movements to account for the observed shape changes. We think, however, that a slightly modified model is more likely to describe the actual intranucleosomal movements. In this model the DNA is coiled on the outside of the nucleosome core with about 80 base pairs per supercoil as has been suggested previously (*11, 27*). As is illustrated in Fig. 10, the 140 base pairs form about two loops in two nearly parallel planes. A dyad or pseudodyad passes between the two planes through the 70th base pair where the two loops are joined. Only this region of the DNA that is common to both loops must remain fixed during a shape change of the nucleosome. Therefore, we postulate the existence of a pivot in this region and explain the conformational variability of the nucleosome by rotations around this pivot (at the origin in Fig. 10). Thus, a change of the wedge angle $\phi$ alters the angle between the planes of the two loops which involves a torsion of the DNA at the pivot. A change of the twist angle $\psi$, on the other hand, is generated by a rotation around an axis nearly perpendicular to these planes. By this movement the DNA is bent (or kinked) or straightened in the region of the pivot. Because the supercoiling of the DNA in the nucleosome is left-handed (*37*), we would obtain a plausible explanation for the absence of left-handed helices in cylinders if we assume that the bending of the DNA at $\psi = 0$ cannot increase further but only decrease.

Another feature of this model is that the largest movements, for a given change of wedge and twist angle, occur opposite to the pivot at the surface of the nucleosome. These movements are twice as large as those calculated above. Thus, the extreme displacements are 26 Å if the twist angle $\psi = 0$, and they are 16 Å if the change of the twist angle is maximal (*38*). Since van der Waals forces do not allow large variations of the bond lengths, it appears likely that the interactions determining the variability of the shape of the nucleosome are electrostatic. This conclusion is supported by the observation that the cylinders dissociate into single nucleosome cores upon elevation of the ionic strength to 0.03 within 10 minutes. The large shape changes and the nearly continuous spectrum of conformations are unusual. We conclude that they are important and probably related to the physiological role of the nucleosome. Since the organization of a particular chromatin region depends on its role at a specific time (for example, during its activation, transcription, replication, polytenization, or recombination), the remarkable conformational variability (*39*) of the nucleosome could provide the freedom necessary for such a dynamic structure.

### Binding Between Nucleosome Cores

The formation of nucleosome arcs and cylinders yields information not only on intranucleosomal movements but also provides insight into internucleosomal interactions. In particular, it implies that the primary association occurs between the top and bottom planes of the nucleosome cores. The constant curvature of an arc suggests that this binding is specific with the pivot on the inside of the arc. It has been shown, however, that, in hexagonal crystals, the nucleosomes form sinusoidal rows by placing the pivot every three nucleosomes on opposite sides (*27*). This second type of top-to-bottom binding is not favored under the conditions of association used in our work. If both types of binding occur in the cell, an additional degree of freedom is gained for the organization of chromatin. Interaction between helices of the same layer could also be specific, whereas binding between concentric arcs or helices of adjacent layers is probably unspecific because in both cases they consist of different numbers of nucleosomes per turn. These types of binding are considerably weaker than the top-to-bottom association of nucleosomes since the helices separate frequently during preparation of the specimens.

Although the arrangements of nucleosome cores in arcs or cylinders differ from the native structure of chromatin, we assume that the interactions and properties of nucleosomes evident from our studies are essential also in native chromatin. Furthermore, since the nucleosome core is conserved (*18, 19, 21*), it might reveal basic elements of inter- and intranucleosomal interactions that are common to the nucleosomes of all organisms. Thus, our results suggest that the strong tendency of nucleosomes to

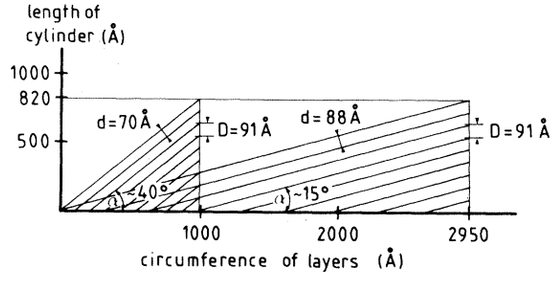


Fig. 8. Squeezing effect. The scheme shows one turn of the unfolded inner- and outermost layers of the cylinder in Fig. 6b. The nine intertwined helices of each layer have an identical pitch but different pitch angles $\alpha$, which results in a squeezing of the helices proportional to cos $\alpha$.

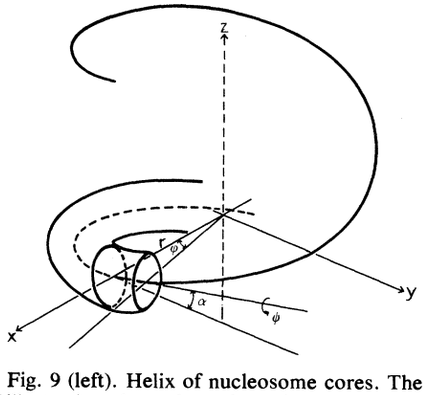


Fig. 9 (left). Helix of nucleosome cores. The illustration shows how the twist angle $\psi$ and the wedge angle $\phi$ of a nucleosome core are related to the radius $r$ and the pitch angle $\alpha$ of the nucleosomal helix.

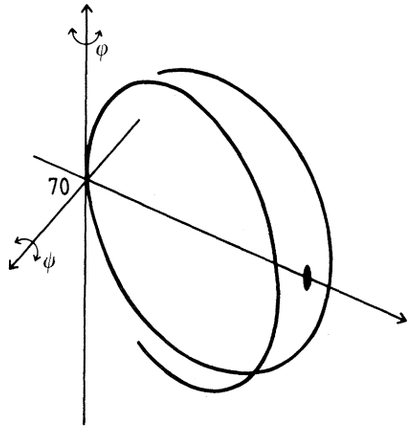


Fig. 10 (right). Model of conformational variability of the nucleosome core. To explain the conformational variability of the nucleosome, a pivot is postulated in the region of the 70th base pair. The two axes of the pivot define with the presumptive dyad of the nucleosome core a Cartesian-coordinate system with its origin at the 70th base pair. Rotations around the two axes of the pivot result in changes of the wedge angle $\phi$ and the twist angle $\psi$ of the nucleosome core. The figure shows only the 140 base pairs of the nucleosome core which have been assumed to form nearly two loops on the outside of the histone octamer (*11, 27*).

associate top to bottom is the basic interaction in the organization of the next level of DNA contraction as, for example, in superbeads or solenoids of nucleosomes (*9*). In this case, H1 or other nonhistone proteins (or a combination) would probably be responsible for the exact organization and stabilization of the superstructure.

### References and Notes


1. J. F. Miescher, Jr., *Collected Works, Edited by His Friends* (Leipzig, 1897).
2. R. Olby, *The Path to the Double Helix* (Univ. of Washington Press, Seattle, 1974).
3. O. T. Avery, C. M. MacLeod, M. McCarty, *J. Exp. Med.* **79**, 137 (1944).
4. J. D. Watson and F. H. Crick, *Nature (London)* **171**, 737 (1953).
5. D. R. Hewish and L. A. Burgoyne, *Biochem. Biophys. Res. Commun.* **52**, 504 (1973).
6. R. D. Kornberg, *Science* **184**, 868 (1974).
7. A. L. Olins and D. E. Olins, *ibid.* **183**, 330 (1974).
8. M. Noll, *Nature (London)* **251**, 249 (1974).
9. J. T. Finch and A. Klug, *Proc. Natl. Acad. Sci. U.S.A.* **73**, 1897 (1976); A. L. Bak, J. Zeuthen, F. H. C. Crick, *ibid.* **74**, 1595 (1977); M. Renz, P. Nehls, J. Hozier, *ibid.*, p. 1879; J. Sedat and L. Manuelidis, *Cold Spring Harbor Symp. Quant. Biol.*, in press.
10. R. D. Kornberg, *Annu. Rev. Biochem.* **46**, 931 (1977).
11. M. Noll, *J. Mol. Biol.* **116**, 49 (1977).
12. J. O. Thomas and R. D. Kornberg, *Proc. Natl. Acad. Sci. U.S.A.* **72**, 2626 (1975); *FEBS Lett.* **58**, 353 (1975).
13. L. A. Burgoyne, D. R. Hewish, J. Mobbs, *Biochem. J.* **143**, 67 (1974).
14. M. Noll, *Nucleic Acids Res.* **1**, 1573 (1974).
15. J. F. Pardon, D. L. Worcester, J. C. Wooley, K. Tatchell, K. E. Van Holde, B. M. Richards, *ibid.* **2**, 2163 (1975); R. P. Hjelm, G. G. Kneale, P. Suau, J. P. Baldwin, E. M. Bradbury, K. Ibel, *Cell* **10**, 139 (1977).
16. J. L. Compton, M. Bellard, P. Chambon, *Proc. Natl. Acad. Sci. U.S.A.* **73**, 4382 (1976).
17. M. Noll and R. D. Kornberg, *J. Mol. Biol.* **109**, 393 (1977); M. Noll, in *Organization and Expression of Chromosomes*, V. G. Allfrey, E. K. F. Bautz, B. J. McCarthy, R. T. Schimke, A. Tissières, Eds. (Dahlem Konferenzen, Berlin, 1976), p. 239; M Noll, in *Nucleic Acid-Protein Recognition*, H. Vogel, Ed. (Academic Press, New York, 1977), p. 139.
18. M. Noll, *Cell* **8**, 349 (1976); N. R. Morris, *ibid.*, p. 357.
19. J. O. Thomas and V. Furber, *FEBS Lett.* **66**, 274 (1976); C. Spadafora, M. Bellard, J. L. Compton, P. Chambon, *ibid.* **69**, 281 (1976); E. M. Johnson, V. C. Littau, V. G. Allfrey, E. M. Bradbury, H. R. Matthews, *Nucleic Acids Res.* **3**, 3313 (1976); D. Lohr, R. T. Kovacic, K. E. Van Holde, *Biochemistry* **16**, 463 (1977).
20. R. D. Todd and W. T. Garrard, *J. Biol. Chem.* **252**, 4729 (1977); A. Prunell and R. D. Kornberg, *Cold Spring Harbor Symp. Quant. Biol.* **42**, 103 (1978).
21. D. Lohr, J. Corden, K. Tatchell, R. T. Kovacic, K. E. Van Holde, *Proc. Natl. Acad. Sci. U.S.A.* **74**, 79 (1977).
22. B. R. Shaw, T. M. Herman, R. T. Kovacic, G. S. Beaudreau, K. E. Van Holde, *ibid.* **73**, 505 (1976).
23. A. J. Varshavsky, V. V. Bakayev, G. P. Georgiev, *Nucleic Acids Res.* **3**, 477 (1976); R. T. Simpson and J. P. Whitlock, *ibid.*, p. 2255.
24. J. T. Finch, M. Noll, R. D. Kornberg, *Proc. Natl. Acad. Sci. U.S.A.* **72**, 3320 (1975).
25. H. H. Ohlenbusch, B. M. Olivera, D. Tuan, N. Davidson, *J. Mol. Biol.* **25**, 299 (1967).
26. This figure was obtained by electron microscopical quantitation using the method of agar filtration in the presence of a known amount of polystyrene spheres [J. Dubochet and E. Kellenberger, *Microsc. Acta* **72**, 119 (1972)].
27. J. T. Finch, L. C. Lutter, D. Rhodes, R. S. Brown, B. Rushton, M. Levitt, A. Klug, *Nature (London)* **269**, 29 (1977).
28. J. P. Langmore and J. C. Wooley, *Proc. Natl. Acad. Sci. U.S.A.* **72**, 2691 (1975).
29. J. F. Pardon, D. L. Worcester, J. C. Wooley, R. I. Cotter, D. M. J. Lilley, B. M. Richards, *Nucleic Acids Res.* **4**, 3199 (1977).
30. J. E. Ladner, J. T. Finch, A. Klug, B. F. C. Clark, *J. Mol. Biol.* **72**, 99 (1972); S. H. Kim, G. Quigley, F. L. Suddath, A. McPherson, D. Sneden, J. J. Kim, J. Weinzierl, A. Rich, *ibid.* **75**, 421 (1973).
31. A. J. Varshavsky and V. V. Bakayev, *Mol. Biol. Rep.* **2**, 247 (1975); C. L. F. Woodcock, J. P. Safer, J. E. Stanchfield, *Exp. Cell Res.* **97**, 101 (1976); A. Engel, J. Dubochet, E. Kellenberger, *J. Ultrastruct. Res.* **57**, 322 (1976).
32. The width of the rows differs slightly from the 110 Å observed for the width of the arcs. This difference is probably due to dehydration of the cylinders.
33. We take $\alpha = 30°$ for the external helices and assume a cylinder consisting of only three layers (no clear cases of cylinders with less than three layers have been observed). The central hole has a diameter of 370 Å, which is the preferred internal diameter of cylinders consisting of thin walls with large external pitch angles.
34. For an unflattened cylinder, the pitch angle $\alpha$ is related to the observed angle $\alpha'$ (defined in Fig. 6b) by the equation $\alpha = \arctan[(2/\pi)\tan\alpha']$ if we assume that the last rows used to measure $\alpha'$ of the innermost layer are part of the same helix (Fig. 6b). Should this assumption be wrong, this equation yields only an estimate for the lower limit of $\alpha$.
35. The derivation of these equations assumes a constant mean height $h$ of the nucleosomes and is based on geometrical considerations. Upon request it may be obtained from us.
36. From Eqs. 2 and 3, estimates for the lower and upper limits of $\phi$ and $\psi$ are obtained. The wedge angle $\phi$ reaches a maximum when $\alpha$ and $r$ are minimal. We cannot measure $\alpha$ directly for the innermost radius of the cylinders, but we may approximate helices with small $\alpha$ by the nucleosome arcs. Consequently, the maximum wedge angle $\phi$ of nucleosomes in cylinders is about 16°. The smallest value of $\phi \simeq 3°$ is found for helices with maximal $r$ which all have a small pitch angle $\alpha$. The twist angle $\psi$ reaches a maximum when $\alpha = 45°$ and $r$ is minimal. It follows that $0 \leq \psi \leq 7°$ (*33*). In addition, we find by division of Eqs. 2 and 3 that $\psi/\phi = \tan\alpha$. Since $\alpha \leq 45°$, it follows that the twist angle $\psi$ is always smaller than or about equal to the wedge angle $\phi$ within the same nucleosome. From the maximum variation of $\phi$ and $\psi$, the largest shape change of a nucleosome may be expressed in terms of the distances by which top and bottom planes move apart $[(d/2)\,\Delta\phi$; $d$ is the diameter of the nucleosome] or are twisted $[(d/2)\,\Delta\psi]$ at the periphery of the nucleosome. Thus we obtain for the extreme distortions $(d/2)\,\Delta\phi \cong 13$ Å, $(d/2)\,\Delta\psi = 0$ and $(d/2)\,\Delta\psi \cong 7$ Å, $(d/2)\,\Delta\phi \cong \lambda 4$ Å.
37. J. E. Germond, B. Hirt, P. Oudet, M. Gross-Bellard, P. Chambon, *Proc. Natl. Acad. Sci. U.S.A.* **72**, 1843 (1975).
38. The values are calculated from $d\Delta\phi \cong 26$ Å, $d\Delta\psi = 0$ and $d\Delta\psi \cong 14$ Å, $d\Delta\phi \cong 8$ Å.
39. Since it is not clear whether external forces are required to induce the conformational changes of the nucleosome, we cannot decide yet whether our tentatively used "conformational variability" or the expressions "conformational flexibility" or "malleability" describe this property of the nucleosome most precisely.
40. M. Noll, J. O. Thomas, R. D. Kornberg, *Science* **187**, 1203 (1975).
41. T. Maniatis, A. Jeffrey, H. van deSande, *Biochemistry* **14**, 3787 (1975).
42. J. Kistler, U. Aebi, E. Kellenberger, *J. Ultrastruct. Res.* **59**, 76 (1977).
43. The hexagonal crystals and the cylinders shrink considerably upon irradiation by the electron beam. Therefore, all length measurements were made at an electron dose below 5 electrons/Å$^2$ which produces negligible contraction. Stacked disk aggregates of tobacco-mosaic virus protein added to the preparation were used as standards. The thickness of a disk was taken as 53.5 Å (J. T. Finch and A. Klug, *J. Mol. Biol.* **87**, 633 (1974).
44. R. W. Horne and I. Pasquali-Ronchetti, *J. Ultrastruct. Res.* **47**, 361 (1974).
45. R. Markham, S. Frey, G. J. Hills, *Virology* **20**, 88 (1963).
46. U. Aebi, R. K. L. Bijlenga, B. ten Heggeler, J. Kistler, A. C. Steven, P. R. Smith, *J. Supramol. Struct.* **5**, 475 (1976).


47. We thank Dr. H. Hengartner for the dialysis chambers used in the association experiments, J. Kistler and Dr. E. Kellenberger for discussions and advice, Dr. S. Artavanis-Tsakonas for comments on the manuscript, and R. Oetterli for photographic work. Swiss National Science Foundation grant 3.719.76 provided support to M.N. Address reprint requests to M.N.